

Influence of Multiwall Carbon Anotubes on Direct Current Electrical Transport and Magnetotransport Properties of Conducting Polymers

G.Chakraborty¹, K.Gupta², A.K.Meikap² and P.C.Jana^{3*}

¹Department of Applied Science & Humanities, Durgapur Institute of Advanced Technology & Management, West Bengal University of Technology, Durgapur-713212, West Bengal, India

²Department of Physics, National Institute of Technology, Durgapur Mahatma Gandhi Avenue, Durgapur – 713 209, West Bengal, India

³Department of Physics and Technophysics, Vidyasagar University, Midnapore- 721102, West Bengal, India.

*Email: pareshjana@rediffmail.com

Received November 1, 2011; accepted December 12, 2011

ABSTRACT

Different conducting polymers – multiwall carbon nanotube composites have been prepared by in-situ chemical polymerization technique. Direct current electrical transport properties of different composites have been investigated in the temperature range $77 \leq T \leq 300\text{K}$ in presence and also in absence of magnetic field up to 1 T. The dc conductivity of the composites follows Mott's variable range hopping theory. The magnetoconductivity of the samples shows a transition from positive to negative value with increasing temperature which can be explained by the dominance of wave function shrinkage effect over quantum interference effect.

Keywords: Polyaniline, Polypyrrole, Multi walled Carbon nanotubes, VRH theory, Charge transport, Conductivity, Magnetoconductivity

1. Introduction

Study of Carbon nanotube (CNT) - conducting polymer composites have become a field of popular and extensive research work due to the advantages of combining organic conductors with nanodimensional systems with interesting physicochemical properties and potentially useful applications [1-3]. They have been considered as a

promising advanced material for many applications such as electromagnetic shielding, organic light-emitting diodes, photovoltaic cells, energy storage devices, sensors, electrostatic dissipation and antennas [4–6]. After the successful preparation of carbon nanotubes and polymer composites by Ajayan et al [7], there have been extensive progresses to combine carbon nanotubes and polymers to produce functional composite materials with desirable electrical and mechanical properties [8-12]. Conducting polymers like Polyaniline (PANI) and polypyrrole (PPy) are important class of polymeric materials due to their relatively high conductivity, better stability, low cost synthesis and easier fabrication procedure. The presence of extended π – conjugation along the polymeric backbone is responsible for higher conductivity of conducting polymers. They are attractive building blocks for the development of novel polymer-nanocomposite materials with enhanced functionality, especially if it comes to enhanced conductivity, thermal stability and reinforcement properties [13-15]. CNT, on the other hand, have a large aspect ratio to make them useful as a reinforced material for enhanced electrical, mechanical and other physical properties of the polymer CNT composites. Although a unique compatibility between conducting polymers and CNT has been shown by the recent studies, any definite conclusions cannot be taken about their temperature and magnetic field dependent electrical conductivity. Very few of the previous reports explain the true mechanism of temperature dependent electrical transport properties and magnetoconductivity of polymer carbon nanotube composites, especially in the below room temperature region. In the present work, in-situ fabrication of HCl doped PANI and PPy with multiwall carbon nanotube (MWCNT) has been done along with an extensive investigation of low temperature ($77 \leq T \leq 300\text{K}$) conductivity and magnetoconductivity (upto 1T) of the different conducting polymer- MWCNT composites.

2. Sample preparation and experimental techniques

2.1 Materials

Aniline, pyrrole, cetyl trimethylammonium bromide (CTAB), MWCNT (Nanocyl 7001) ammonium peroxydisulphate (APS), ethanol and acetone were used as received from the market and purified. Double distilled water has been used in this investigation.

2.2 Synthesis

Composites of polyaniline and polypyrrole with MWCNT have been synthesized by in situ chemical oxidative polymerization using CTAB as a surfactant. 1.136 gm CTAB and 60 mg MWCNT have been added in 300 ml 1(M) HCl and the mixture had been sonicated to obtain a well-dispersed suspension. It was then kept at $0-5^{\circ}\text{C}$ in the refrigerator. A precooled 1.2 ml aniline and 125 ml 1(M) HCl containing 2.7 gm APS had been added sequentially to the MWCNT-CTAB suspension taken in an ice chamber with continuous magnetic stirring for 1 hr and then left standing in the refrigerator at $0-5^{\circ}\text{C}$ for 24 hr. A black precipitate had been obtained on filtration. The solid mass had been washed with ethanol and

acetone repeatedly to remove oligomers and unreacted monomer. Then washed with double distilled water several times and dried at room temperature in a dynamic vacuum for 24 hr. Same technique had been taken for the preparation of Polypyrrole-MWCNT composites. For comparison purposes, two reference samples of Polyaniline and Polypyrrole without MWCNT had been prepared.

2.3 Characterization

The electrical conductivity of the samples was measured by a standard four probe method after good contact was ensured with highly conducting graphite adhesive (Electrodag 5513, Acheson, Williston, VT) and fine copper wires as the connecting wires. The dc conductivity was measured with an 8¹/₂ – digit Agilent 3458A multimeter. The temperature dependence of the conductivity was studied with a liquid nitrogen cryostat. For the control and measurement of the temperature, an ITC 502S Oxford temperature controller was used. To measure the dc response, pellets of 1 cm in diameter of the samples was made by pressing the powder under a hydraulic pressure of 500 MPa. The magnetoconductivity was measured in the same manner by the variation of the transverse magnetic field ($B < 1$ T) with an electromagnet.

3. Results and discussion

3.1 D.C. Conductivity

To investigate the direct current charge transfer mechanism of the different conducting polymer-MWCNT composites, the variation of conductivity of the samples have been measured with temperature within a range $77 \leq T \leq 300\text{K}$. The room temperature conductivity ($\sigma_{300\text{K}}$) of the different samples is indicated in table-1. The values indicate an enhancement in conductivity with the introduction of MWCNT in polymer matrix. Maximum conductivity is obtained for the PPy-MWCNT composite. Conducting polymers are considered as a good electron donor whereas MWCNT are relatively good electron acceptors. So the interaction between the quinoid rings of conducting polymers and MWCNT facilitates the charge transfer process between the two components. The presence of a large π -conjugated structure in MWCNT results in a high localization length of around 10nm [16] and hence has a high conductivity. On the other hand, crystalline and amorphous conducting polymer has smaller localization length resulting in a poor conductivity. Thus, due to the strong coupling between the MWCNTs and the polymer chains increases the average localization length and hence an increase in conductivity for the composite samples compared to pure conducting polymers. The variation of conductivity as a function of temperature is shown in Fig. 1. The semiconducting nature of all the investigated samples can be observed for their increase in conductivity with increasing temperature. This happens due to increase in the charge transfer process between conducting polymers and MWCNT with increasing temperature. Generally, the temperature dependence of conductivity of a disordered semiconducting system are explained in terms of Mott's variable range hopping (VRH) model [17], according to which, the conductivity can be expressed as

$$\sigma(T) = \sigma_0 \exp \left[- \left(\frac{T_{Mott}}{T} \right)^\gamma \right] \quad (1)$$

where the VRH exponent γ determines the dimensionality of the conducting medium by the relation $\gamma = \frac{1}{1+d}$. For three, two and one dimensional system, the possible values of γ is $1/4$, $1/3$, and $1/2$ respectively. σ_0 is the resistivity at infinite temperature; T_{Mott} is the Mott characteristic temperature depending on the electronic structure, and the energy distribution of the localized states and can be written as

$$T_{Mott} = \frac{16}{k_B N(E_F) L_{loc}^3} \quad (2)$$

where k_B is the Boltzmann constant, $N(E_F)$ is the density of states at the Fermi level and L_{loc} is the localization length.

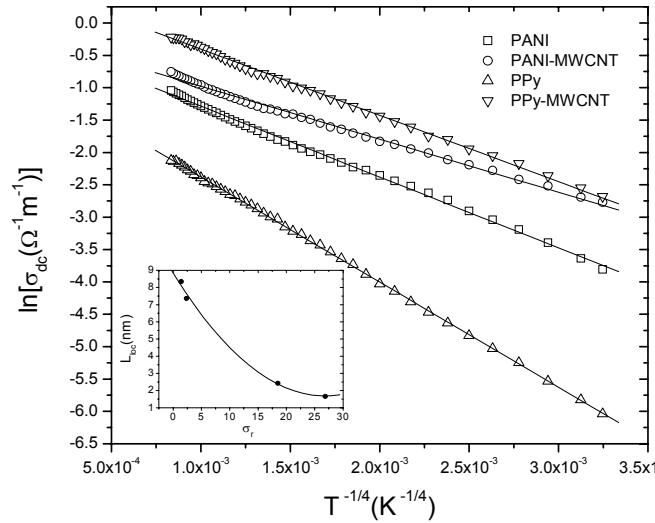


Fig.1: Temperature dependence of the dc conductivity of different conducting polymer and conducting polymer –MWCNT composites. The solid lines are fitted to eq. (1). Inset shows the variation of localization length (L_{loc}) with conductivity ratio(σ_r)

The proper charge transfer mechanism of all the investigated samples can be obtained from the temperature dependence of dc conductivity which has been analyzed by Eq. (1). A graph has been plotted between $\ln[\sigma_{dc}(T)]$ with $T^{-1/4}$ for all the samples which shows a linear behaviour for all the samples throughout the entire

range of investigating temperature ($77 \leq T \leq 300\text{K}$). T_{Mott} has been calculated from the slopes of these variations in Fig.1 and are indicated in table-1 for different samples. The value of T_{Mott} is strongly influenced by the disorder present in the sample, which in turn, is expressed in terms of the conductivity ratio, indicated in table-1. The value of disorder increases with increase in the conductivity ratio. The higher value of $\sigma_r (=26.86)$ for pure polypyrrole indicates the presence of more disorder in that sample. So, a higher value of T_{Mott} is obtained in case of pure polypyrrole. The results obtained in the present investigation indicate that 3-D transport is the dominating charge transport mechanism. The variation of localization length with conductivity ratio is shown in the inset of Fig.1. There is a decrease in localization length with increasing σ_r . For higher disorder, the electronic wavefunctions are localized in a smaller region results a decrease in localization length and hence, localization length decreases with increasing σ_r . Thus, the disorder present in the sample has a strong influence on the localization length.

3.2 D.C. Magnetoconductivity

The magnetic field dependent conductivity of the different samples has been measured within a temperature range 77-300K and under a transverse magnetic field upto 1 Tesla. The variation of magnetoconductivity with magnetic field strength at $T=300\text{K}$ for different samples are shown in Fig.8. All the samples show negative magnetoconductivity at room temperature i.e. their conductivity decreases with increasing magnetic field strength. The maximum percentage changes of

conductivity $\left[\frac{\sigma(B, T) - \sigma(0, T)}{\sigma(0, T)} \times 100 \right]$ under a magnetic field of 0.8 Tesla at

300K are indicated in table-1. In general, the dc magnetoconductivity can be analyzed in terms of simple phenomenological model that consists of two simultaneously acting hopping processes- the wave function shrinkage model [18-19] and the forward interference model (Quantum interference effect)[20-22]. In wave function shrinkage model, the average hopping length reduces due to the contraction of wave function of electrons under the influence of a magnetic field. As a result, the conductivity decreases with increasing magnetic field. Under a small magnetic field, the magnetoconductivity ratio can be expressed as [18]

$$\ln \left[\frac{\sigma(B, T)}{\sigma(0, T)} \right] = -t_1 \frac{e^2 L_{\text{loc}}^4}{\hbar^2} \left(\frac{T_{\text{Mott}}}{T} \right)^{3/4} B^2 \quad (3)$$

where $t_1 = 5/2016$ and L_{loc} is the localization length. Again in forward interference model, direct and indirect hopping mechanisms between localized states are considered, and the phase factor that is considered by the field flux through the area between the hopping routes is averaged to show that field reduces the resistance,

resulting in positive magnetoconductivity. According to this model, the magnetoconductivity ratio becomes

$$\frac{\sigma(B, T)}{\sigma(0, T)} = 1 + \frac{\frac{C_{sat} B}{B_{sat}}}{1 + \frac{B}{B_{sat}}} \quad (4)$$

where C_{sat} is a temperature independent parameter and

$B_{sat} = 0.7 \left(\frac{\hbar}{e} \right) \left(\frac{8}{3} \right)^{\frac{3}{2}} \left(\frac{1}{L_{loc}} \right)^2 \left(\frac{T}{T_{Mott}} \right)^{\frac{3}{8}}$. It was observed that due to the small

localization length of conducting polymers, the average hopping length

$R_{hop} = \left(\frac{3}{8} \right) \left(\frac{T}{T_{Mott}} \right)^{\frac{1}{4}} L_{loc}$ is small and wave function shrinkage effect is

observed [41]. However, a large positive magnetoconductivity for CNT films or pellets at weak magnetic field due to their large L_{loc} and R_{hopp} is found in the literature [23-24]. Therefore, the sign and magnitude of magnetoconductivity of the conducting polymer-MWCNT composites are changed due to the competition of these two (wave function shrinkage and quantum interference) effects. The observed decrement of magnetoconductivity of the investigated samples indicates the predominance of wave function shrinkage effect over quantum interference effect. So the measured data has been analyzed according to the wave function shrinkage model. Fig.2 shows the linear variation of $\ln[\sigma(B, T)/\sigma(0, T)]$ with B^2 for different samples at room temperature. The points in the graph represent the experimental data and the curves represent the theoretical best fits according to the wave function shrinkage model. It is evident from Fig.2 that the experimental data are fitted reasonably well with the presumed theoretical model. Localization length has been calculated from the slopes of the graphs of Fig.2 using Eq.(3). The variation of magnetoconductivity of PPy-MWCNT composites with magnetic field is shown in Fig.3 at different but constant temperatures. A change in magnetoconductivity from positive to negative is observed at different temperatures. In Fig.3, the points are the experimental data and the curve is the theoretical best fit with wave function shrinkage model. The data are reasonably well fitted with the theoretical curves showing that the magnetotransport at different temperatures are in accordance with the wave function shrinkage effect. All the other samples show a similar behavior. The average hopping length at different temperatures has been calculated from the known values of L_{loc} (obtained from the slopes of the graphs in Fig.2) and T_{mott} . The variation of average hopping

length with temperature for different samples is shown in Fig.4 which shows a decrease in R_{hopp} with increasing temperature.

Table 1: Different physical parameters of samples: Conductivity at room temperature ($\sigma(300\text{K})$), Conductivity ratio (σ_r), temperature exponent (γ), Mott characteristic temperature (T_{Mott}), Percentage change in magnetoconductivity, localization length (L_{loc}), Average hopping length (R_{Hopp}).

Parameters	PPy	PANI	PANI-MWCNT	PPy-MWCNT
$\sigma_{300} (\Omega^{-1} \text{m}^{-1})$	0.02	0.35	0.47	0.85
$\sigma_r = \sigma_{300}/\sigma_{77}$	26.86	18.47	2.35	1.4
γ	0.25	0.25	0.25	0.25
$T_{\text{mott.}}(\text{K})$	2.72×10^8	2.43×10^7	5.93×10^6	3.62×10^6
$[\sigma(B)-\sigma(0)/\sigma(0)] \times 100$	-0.07	-0.39	-0.67	-0.86
$(L_{\text{loc}})300(\text{nm})$	1.67	2.43	7.36	8.35
$R_{\text{hopp}}(\text{nm})$	0.017	0.058	0.172	0.273

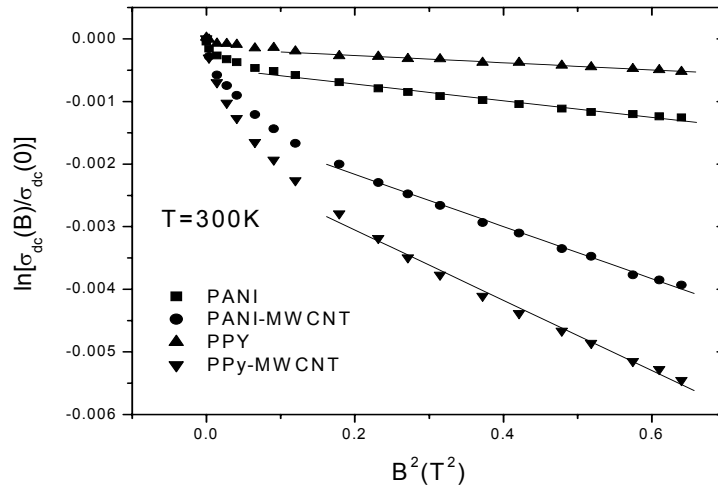


Fig.2: Variation of the dc magnetoconductivity with perpendicular magnetic field of different conducting polymer and conducting polymer–MWCNT composites at 300 K [the solid lines are fitted to eq. (3)].

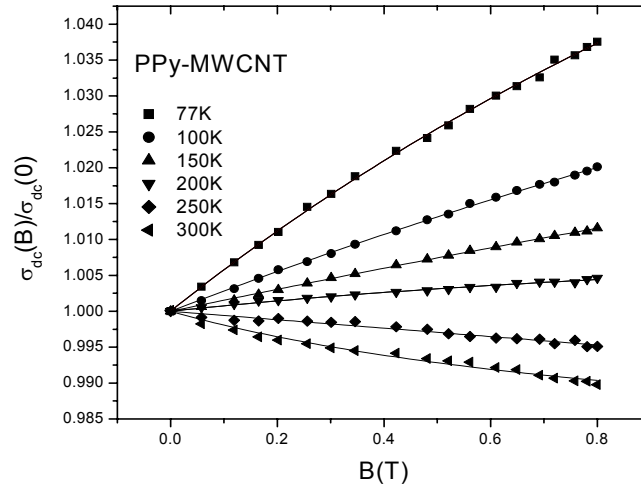


Fig.3: Variation of the dc magnetoconductivity with perpendicular magnetic field of the polypyrrole-MWCNT composite at different temperatures. The solid lines are fitted to Eq.(4).

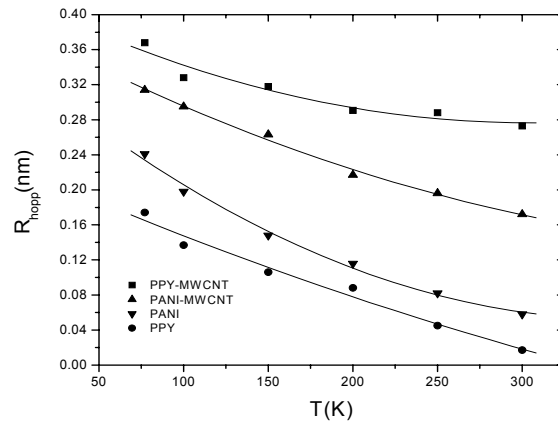


Fig.4: Variation of average hopping length (R_{hopp}) with Temperature for different investigated samples.

4. Conclusion

The overall conductivity of the polymer-MWCNT composites becomes higher than pure polymers. 3-D VRH model is followed by all the investigated samples. The room temperature magnetoconductivity of the samples are negative due to small average hopping length, which can be interpreted by wave function shrinkage effect. A transition from positive to negative magnetoconductivity is observed for all the samples due to the dominance of wave function shrinkage effect over quantum

interference effect. The average hopping length decreases with increasing temperature.

Acknowledgements

The authors gratefully acknowledge the principal assistance received from the MHRD, Government of India during this work.

REFERENCES

1. H.S. Woo, R. Czerw, S. Webster, D.L. Carroll, J.W. Park, J.H. Lee, *Synth. Met.* 116 (2001) 369.
2. H.Ago, K. Petritsch, M.S.P. Shaffer, A. H. Windle, R.H. Friend, *Adv. Mater.* 11 (1999)1281.
3. E. Bekyarova, M. Davis, T. Burch, M.E. Itkis, B. Zhao, S. Sunshine, R.C. Haddon, *J. Phys. Chem. B* 108 (2004) 19717.
4. H Naarman, *Science and Application of Conducting Polymers*, Adam Hilger, Bristol, 1991
5. D A Seanor, *Electronic Properties of Polymer*, Academic, New York, 1992.
6. T.A.Skotheim, R.L.Elsenbaumer, J. R. Reynolds (Eds.) *Hand Book of Conducting Polymers* (Marcel Dekker Inc., New York, (1998) p.945
7. P M Ajayan, O Stephan, C Colliex, D Trauth *Science* 365 (1993)1212.
8. E T Thostenona, Z Renb, T W Choua *Composite Sci. Technol.* 61 (2001) 1899.
9. R H Baughman, A A Zakhidov, W A Heer *Science* 297 (2002) 787.
10. E Kymakis, G A Amaratunga *J. Appl. Phys. Lett.* 80 (2002) 112.
11. K. Takahashi, K. Nakamura, T. Yamaguchi, T. Komura, S. Ito, R. Aizawa, K. Murata, *Synth. Met.* 128 (2002) 27.
12. B. Zhao, H. Hu, R.C. Haddon, *Adv. Funct. Mater.* 14 (2004) 71.
13. S A Curran, P M Ajayan, W J Blau, D L Carroll, J N Coleman, A B Dalton, A P Davey, A Drury, B Mccarthy, S Maier, A Strevens, *Adv. Mater* 10 (1998)1091.
14. M Cochet, W K Maser, A M Benito, M A Callejas, M T Martinez, J M Benoit, J Schreiber, O Chauvet *Chem. Comm.* (2001)1450.
15. H Zengin, W Zhou, J Jin, R Czerw, Jr D W Smith, L Echegoyen, D L Carroll, S H Foulger, J Ballato *Adv. Mater* 14 (2002)1480.
16. J. Joo, S. M.Long, J. P.Pouget, E. J.Oh, A.G.MacDiarmid, A. J. Epstein, *Phys Rev B* 57 (1998) 9567.
17. N. F.Mott, E.Davis, *Electronic Process in Noncrystalline Materials*, 2nd ed.; Clarendon Press: Oxford, 1979.
18. B. L. Shklovskii, *Sov Phys Semicond* 17 (1983) 1311.
19. B. L. Shklovskii, A. L. Efros, *Electronic Properties of Doped Semiconductors*; Springer: Berlin, 1994, p 202.

20. V. L. Nguyen, B. Z. Spivak, B. I. Shklovskii, *Sov Phys JETP* 62 (1995) 1021.
21. U.Sivan, O. Entin-Wohiman, Y. Imry, *Phys Rev Lett* 60 (1988) 1566.
22. R.Rosenbaum, A. Milner, S.Hannens, T. Murphy, E. Palm, B. Brandt, *Physica B* 294–295 (2001) 340.
23. M. S. Fuhrer, W. Holmes, P. L. Richards, P. Delaney, S. G. Louie, A. Zettl, *Synth Met* 103 (1999) 2529.
24. Y.Yosida, I. Oguro, *J Appl Phys* 86 (1999) 999.